Food Chemistry 155 (2014) 31–37

Contents lists available at ScienceDirect

Food Chemistry

journal homepage: www.elsevier.com/locate/foodchem

Baeckeins F–I, four novel *C*-methylated biflavonoids from the roots of *Baeckea frutescens* and their anti-inflammatory activities

Bei-Xi Jia [a,b,*], Xian-Lei Zeng [a], Feng-Xiao Ren [c], Lu Jia [a], Xiao-Qing Chen [b], Jie Yang [b], Hong-Min Liu [a,*], Qiang Wang [b,*]

[a] Department of Pharmacognosy, College of Pharmacy, Zhengzhou University, No. 100 of Science Road, Zhengzhou 450001, PR China
[b] State Key Laboratory of Natural Medicines, China Pharmaceutical University, No. 24 Tongjia Lane, Nanjing 210009, PR China
[c] Henan Zhongshuai Pharmaceutical Science and Technology Development Co., Ltd, Zhengzhou 450001, PR China

ARTICLE INFO

Article history:
Received 5 November 2013
Received in revised form 4 January 2014
Accepted 11 January 2014
Available online 24 January 2014

Keywords:
Baeckea frutescens
C-methylated biflavonoid
Baeckeins F–I
Absolute configuration
Anti-inflammatory activity

ABSTRACT

Baeckea frutescens is an aromatic shrub used in South China as an ornamental and as a spice. Four unusual *C*-methylated biflavonoids named baeckeins F–I (**1**–**4**) were isolated from the roots of *B. frutescens*. The baeckeins F–I possessed a unique carbon skeleton, a flavonol conjugated with a coumaronochromone molecule *via* the unusual linkages of C-2–C-8* and C-3–O–C-7*. Their structures were elucidated by analysis of the 1D ($^1H/^{13}C$) and 2D NMR (HSQC/HMBC/NOESY) and HR-ESI-MS spectroscopic data, and the absolute stereochemistry for chiral carbons of C-2 and C-3 was established by CD spectrometry combined with quantum chemical calculations. Baeckeins F–I (**1**–**4**) were also evaluated for their anti-inflammatory activities by detecting the NO production of LPS-induced RAW264.7 murine macrophage cell line; baeckein I (**4**) with the β-D-glucose unit and configuration of (2*R*,3*R*) exhibited the highest NO inhibitory activity (IC_{50} = 15.2 μM), which was similar to that of the positive control indomethacin.

1. Introduction

Baeckea frutescens L. (Myrtaceae) is distributed from Southeast Asia to Australia. As an economic crop, *B. frutescens* is widely cultivated in the southern part of China. This aromatic low-growing shrub is not only used as an ornamental plant, but also as an important spice. During recent years, this plant has been collected for a daily health tea known as "Gang-Song-Cha" receiving considerable attention.

There have been previous studies on *B. frutescens* essential oil (Jantan et al., 1998; Tam et al., 2004), sesquiterpenes (Tsui & Brown, 1996a), phloroglucinols (Fujimoto, Usui, Makino, & Sumatra, 1996), chromones (Satake et al., 1999; Tsui & Brown, 1996b), flavonoids (Kamiya & Satake, 2010; Makino & Fujimoto, 1999; Quang, Cuong, Minh, & Kiem, 2008; Tsui & Brown, 1996c) and their derivatives. Amongst these constituents, the total flavonoids have been regarded as the main bioactive components, exhibiting significant anti-inflammatory effects on xylene-induced ear swelling in mice and increased antioxidant activities of the superoxide dismutase (SOD) and glutathione peroxidase (GSH-Px) (Pan, Li, Liao, & Lin, 2012).

Preliminary phytochemical investigations of *B. frutescens* in our laboratory led to the isolation of seven *C*-methylated flavonoids and bioflavonoids; their cytoprotective effects on H_2O_2-induced oxidative cell death in PC12 cells were also evaluated (Jia, Yang, et al., 2011; Jia, Zhou, et al., 2011). To our knowledge, *C*-methylated flavonoids are not widely distributed, but regularly occur in the Myrtaceae family, such as *Eucalyptus*, *Leptospermum*, *Eugenia*, *Lophostemon*, *Syncarpia*, *Angophora*, *Syzygium*, *Agonis*, *Callistemon*, and *Cleistocalyx* (Gottlieb, Da Silva, & Maia, 1972; Mayer, 1990; Rao & Rao, 1991; Wollenweber, Wehde, Dörr, Lang, & Stevens, 2000). These findings suggest that *C*-methylated flavonoids might be distinct to Myrtaceae.

As part of our continuing search for structurally interesting and bioactive *C*-methylated flavonoids, four novel *C*-methylated biflavonoids named baeckeins F–I (**1**–**4**) were isolated from the roots of *B. frutescens* (Fig. 1). In this paper, the structures of the isolates were elucidated by 1D ($^1H/^{13}C$) and 2D nuclear magnetic resonance (NMR) (HSQC/HMBC/NOESY) and high-resolution electrospray ionisation (HR-ESI) mass spectral data, and the absolute configurations were determined by circular dichroism (CD) spectrometry combined with quantum chemical calculations. Furthermore, the anti-inflammatory activities for compounds **1**–**4** were evaluated by detecting nitric oxide (NO) production of lipopolysaccharides (LPS)-induced RAW264.7 murine macrophage cell line.

* Corresponding authors. Address: Department of Pharmacognosy, College of Pharmacy, Zhengzhou University, No.100 of Science Road, Zhengzhou 450001, PR China. Tel.: +86 371 67781891; fax: +86 371 67781908 (B.-X. Jia). Tel.: +86 371 67781905; fax: +86 371 67781908 (H.-M. Liu). Tel.: +86 25 83271390; fax: +86 25 85301528 (Q. Wang).

E-mail addresses: jiabeixi_2003_123@163.com (B.-X. Jia), liuhm@zzu.edu.cn (H.-M. Liu), qwang49@163.com (Q. Wang).

0308-8146/$ - see front matter
http://dx.doi.org/10.1016/j.foodchem.2014.01.022

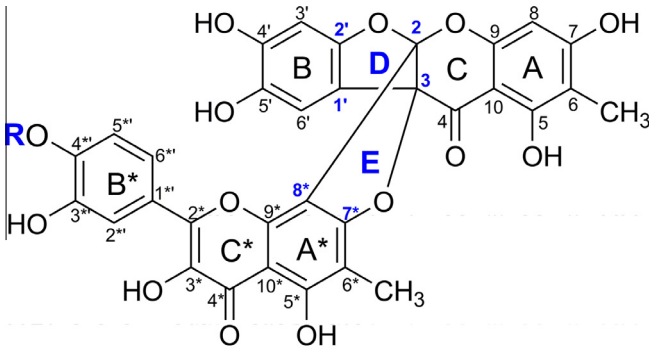

Fig. 1. Structures of compounds **1**–**4**.

2. Materials and methods

2.1. Plant material

The roots of *B. frutescens* were collected from the mountainous areas of Nanning, Guangxi Province, China, and identified by Prof. Qiang Wang of China Pharmaceutical University. A voucher specimen (No. GS001) was deposited in the Department of Chinese Materia Medica Analysis, China Pharmaceutical University, Nanjing, China.

2.2. General experimental procedures

Column chromatography (CC) was carried out using silica gel (SiO_2, 100–200 mesh and 200–300 mesh; Qingdao Haiyang Chemical Co., Ltd., Qingdao, China), RP-C_{18} (40–63 μM; Fuji, Japan) and Sephadex LH-20 (20–100 μM; Pharmacia, Uppsala, Sweden). Thin-layer chromatography (TLC) was performed on precoated silica gel GF_{254} plates (Qingdao Haiyang Chemical Co., Ltd., Qingdao, China) and spots were visualised under the UV light (254 or 365 nm) or detected by spraying $AlCl_3$-EtOH (1%) solution. $^1H/^{13}C$ NMR spectra were recorded in DMSO-d_6 solvent at room temperature on a Bruker AV-500 NMR instrument (^1H at 500 MHz and ^{13}C at 125 MHz; Bruker, Karlsruhe, Germany) with tetramethylsilane (TMS) as the internal standard. 2D-NMR spectra (HSQC/HMBC/ROESY) were obtained at 303 K using the standard Bruker pulse programs. ESI and HR-ESI mass spectral data were acquired on an Agilent 1100 Series LC/MSD ion trap mass spectrometer and an Agilent 6530 LC-Q-TOF/MS instrument (Agilent Technologies, Santa Clara, CA), respectively. Gas chromatography (GC) analysis was carried out on an Agilent 6890 Plus gas chromatograph (Agilent Technologies) using a DB-5 capillary column (30 m × 0.25 mm, i.d.). UV spectra were recorded with a Shimadzu-UV-2450 UV/VIS spectrophotometer (Shimadzu, Tokyo, Japan). IR spectra (KBr disks, cm^{-1}) were determined with the Bruker Tensor 27 spectrometer. CD spectra were obtained on the Jasco J-810 circular dichroism spectrometer (Jasco, Tokyo, Japan). Optical rotations were measured in CH_3OH at 23 °C with a Jasco P-1020 polarimeter. All solvents used were of analytical grade.

2.3. Extraction and isolation

Air-dried and crushed roots of *B. frutescens* (10.0 kg) were extracted with 90% ethanol (30.0 L × 3) at 80 °C for 3 h and concentrated in vacuum to give a total extract of 600 g, which was suspended in water and partitioned with petroleum ether (60–90 °C), ethyl acetate (EtOAc) and *n*-butanol successively. The EtOAc soluble part (204 g) was first subjected to silica gel CC (200–300 mesh, 120 × 10 cm, i.d.) and eluted with a gradient of $CHCl_3/CH_3OH$ (MeOH) (1:0 → 1:1) to yield eight fractions (Fr.1–Fr.8) on the basis of TLC analysis. Fr. 4 (21.6 g) was then submitted to SiO_2 CC (200–300 mesh, 60 × 5 cm, i.d.; $CHCl_3$/MeOH, 50:1 → 10:1) to give five subfractions (Fr.4-1–Fr.4-5), of which Fr.4-1 (2.5 g) was further submitted to a Sephadex LH-20 column (120 × 2 cm, i.d., $CHCl_3$/MeOH, 1:1) to obtain a mixture of compounds **1** and **2** (0.85 g). The mixture was repeatedly chromatographed over RP-C_{18} (60 × 2.5 cm, i.d., MeOH/H_2O, 70:30) to yield compounds **1** (25.1 mg) and **2** (20.6 mg). Part of Fr.6 (2.1 g) was submitted to a Sephadex LH-20 column (120 × 2 cm, i.d.) eluted with $CHCl_3$/MeOH (1:1) to afford six subfractions (Fr.6-1–Fr.6-6), of which Fr.6-2 (0.68 g) was then subjected to repeated CC (Sephadex LH-20, 120 × 2 cm, i.d., MeOH) to obtain mixed compounds **3** and **4**. This mixture was separated by repeated CC (RP-C_{18}, 60 × 2.5 cm, i.d., MeOH/H_2O, 63:37) to obtain compounds **3** (15.0 mg) and **4** (25.7 mg). The detailed flow chart is shown in Fig. S01.

2.3.1. Baeckein F (*1*)

Yellow amorphous powder: $[\alpha]_D^{24}$ +137.6° (*c* = 0.10, MeOH); UV (MeOH) nm λ_{max} (log ε): 238 (2.98), 307 (3.45), 383 (2.78) nm; IR (KBr) ν_{max} 3398, 1636, 1463, 1318, 1183, 1120, 817 cm^{-1}; CD (CH_3CN) λ ($\Delta\varepsilon$) 211 (+8.05), 233 (+5.60), 260 (−2.12), 304 (−23.79), 379 (+9.50) nm; For ^1H and ^{13}C NMR (500 and 125 MHz, DMSO-d_6) spectroscopic data, see Table 1; HR-ESI-MS (positive mode) *m*/*z* 629.0922 $[M+H]^+$ (calcd for $C_{32}H_{21}O_{14}$, 629.0926) (Figs. S02–S08).

2.3.2. Baeckein G (*2*)

Yellow amorphous powder: $[\alpha]_D^{24}$ −215.6° (*c* = 0.11, MeOH); UV (MeOH) nm λ_{max} (log ε): 240 (2.96), 306 (3.45), 380 (2.78) nm; IR (KBr) ν_{max} 3397, 1635, 1465, 1320, 1187, 1119, 813 cm^{-1}; CD (CH_3CN) λ ($\Delta\varepsilon$) 211 (−8.69), 233 (−6.85), 260 (+2.27), 303 (+24.67), 374 (−10.87) nm; For ^1H and ^{13}C NMR (500 and 125 MHz, DMSO-d_6) spectroscopic data, see Table 1; HR-ESI-MS (negative mode) *m*/*z* 627.0794 $[M-H]^-$ (calcd for $C_{32}H_{19}O_{14}$, 627.0780) (Figs. S09–S14).

2.3.3. Baeckein H (*3*)

Yellow amorphous solid: $[\alpha]_D^{25}$ +145.4° (*c* = 0.10, MeOH); UV (MeOH) nm λ_{max} (log ε): 228 (2.87), 308 (3.50), 380 (2.31) nm; IR (KBr) ν_{max} 3397, 1635, 1508, 1463, 1321, 1186, 1070, 813 cm^{-1}; CD (CH_3CN) λ ($\Delta\varepsilon$) 211 (+27.63), 232 (+19.10), 260 (−7.28), 304 (−35.68), 375 (+14.25) nm; For ^1H and ^{13}C NMR (500 and 125 MHz, DMSO-d_6) spectroscopic data, see Table 1; HR-ESI-MS (negative mode) *m*/*z* 789.1313 $[M-H]^-$ (calcd for $C_{38}H_{29}O_{19}$, 789.1308) (Figs. S15–S21).

2.3.4. Baeckein I (*4*)

Yellow amorphous solid: $[\alpha]_D^{25}$ −223.8° (*c* = 0.11, MeOH); UV (MeOH) nm λ_{max} (log ε): 230 (2.83), 307 (3.48), 381 (2.29) nm; IR (KBr) ν_{max} 3385, 1636, 1508, 1463, 1323, 1186, 1069, 802 cm^{-1}; CD (CH_3CN) λ ($\Delta\varepsilon$) 211 (−24.84), 233 (−19.58), 260 (+6.48), 304 (+35.24), 374 (−15.52) nm; For ^1H and ^{13}C NMR (500 and 125 MHz, DMSO-d_6) spectroscopic data, see Table 1; HR-ESI-MS (positive mode) *m*/*z* 791.1455 $[M+H]^+$ (calcd for $C_{38}H_{31}O_{19}$, 791.1454) (Figs. S22–S28).

2.4. Acid hydrolysis and GC analysis

Compounds **3** and **4** (2.0 mg of each) were hydrolysed with 10% HCl-dioxane (1:1, v/v, 5.0 ml) at 80 °C for 4.0 h. The biflavonoid aglycone in the mixture was extracted with EtOAc (5.0 ml × 3), and the sugar component in the aqueous layer was evaporated under reduced pressure. The obtained sugar residue was divided into

Table 1
^{1}H and ^{13}C-NMR data for compounds **1**–**4**; δ-ppm (*J*-Hz).

Position	**1**		**2**		**3**		**4**	
	δ_H	δ_C	δ_H	δ_C	δ_H	δ_C	δ_H	δ_C
2		111.6		111.6		111.6		111.8
3		93.8		93.8		93.8		94.0
4		181.0		181.0		181.1		181.3
5		161.6		161.4		161.6		161.8
6		105.6		105.6		105.7		105.8
CH_3-6	1.86 s	6.9	1.85 s	6.9	1.83 s	6.9	1.85 s	7.0
7		167.7		167.7		167.4		167.5
8	6.18 s	96.3	6.05 s	96.7	6.13 s	96.2	6.20 s	96.3
9		156.8		156.8		156.8		157.0
10		100.0		99.8		100.2		100.3
1'		115.2		115.2		115.1		115.2
2'		149.0		149.0		149.1		149.2
3'	6.64 s	98.9	6.58 s	98.8	6.61 s	98.9	6.68 s	98.8
4'		150.4		150.4		150.5		150.6
5'		142.1		142.0		142.1		142.3
6'	7.09 s	110.1	7.02 s	110.0	7.05 s	110.0	7.13 s	110.1
2*		147.2		147.1		146.2		146.3
3*		136.4		136.3		137.2		137.3
4*		176.0		176.0		176.3		176.4
5*		161.4		161.4		161.5		161.7
6*		102.5		102.4		102.6		102.8
CH_3-6*	2.05 s	7.2	2.00 s	7.2	2.00 s	7.2	2.04 s	7.3
7*		160.3		160.2		160.3		160.4
8*		102.9		103.0		102.9		103.0
9*		148.2		148.2		148.4		148.6
10*		105.0		104.9		105.0		105.2
1*'		122.0		122.0		125.2		125.4
2*'	7.12 d (8.7)	116.0	7.06 d (8.7)	116.0	7.44 d (8.7)	116.2	7.50 d (8.7)	116.4
3*'		145.4		145.4		147.0		146.8
4*'		148.3		148.3		147.3		147.5
5*'	8.10 d (2.0)	115.6	8.04 d (2.0)	115.5	8.10 d (2.0)	115.3	8.12 d (2.0)	115.5
6*'	7.90 dd (8.7, 2.0)	119.5	7.85 dd (8.7, 2.0)	119.5	7.96 dd (8.7, 2.0)	119.4	8.03 dd (8.7, 2.0)	119.6
Glc-1''					4.94 d (7.0)	101.6	5.03 d (6.9)	101.7
2''					3.39 m	73.3	3.46 m	73.5
3''					3.45 m	77.2	3.54 m	77.4
4''					3.23 m	69.8	3.32 m	70.0
5''					3.34 m	75.9	3.43 m	76.0
6''					3.54 dd (11.2, 5.0)	60.7	3.61 dd (11.1, 5.1)	61.0
					3.79 dd (11.3, 2.0)		3.85 dd (11.0, 2.0)	

two halves. One half was identified by SiO_2 TLC with $CHCl_3$/MeOH/H_2O (8:5:1) by comparison with the authentic sample, and the other half was dissolved in dry pyridine (1.0 ml) and L-cysteine methyl ester hydrochloride (2.0 mg) was added, followed by heating at 60 °C for 2 h. Finally, the resulting solution was extracted with cyclohexane and H_2O, and the combined organic phase was analysed by GC with FID detector and the DB-5 capillary column (30 m × 0.25 mm, i.d.). The temperatures for injection and detector were 250 and 280 °C, respectively. The initial temperature of 180 °C was maintained for 5.0 min and then raised to 260 °C at 8 °C/min, and He was used as the carrier gas (Hao et al., 2008; Tang et al., 2005). The standard D-glucose (Sigma–Aldrich, St. Louis, MO) was subjected to the same reaction and GC analysis under the same conditions, and gave a single peak at 12.174 min.

2.5. Computational details

The Q-Chem programme package and the Chem three-dimensional software were employed for CD calculations. The conformation searching was performed at MM2 molecular mechanics force field with the Omega 2.1 programme to afford the dominating conformers. All of the ground-state geometries were optimised at the B3LYP/6-31G+ (d,P) level, and harmonic vibrational frequencies were calculated to confirm their stabilities. The time-dependent density-functional theory (TD-DFT) calculations for excitation energy and rotatory strength *R* were performed at the same level in the gas phase, and then ECD spectra were simulated by overlapping Gaussian functions for each transition (Frisch et al., 2010).

2.6. Anti-inflammatory assay

2.6.1. Cell viability

Murine macrophage cell line RAW264.7 was cultured in plastic dishes containing Dulbecco's Modified Eagle Medium (DMEM; Sigma–Aldrich) supplemented with 10% fetal bovine serum (FBS; Sigma–Aldrich) in a CO_2 incubator (5% CO_2) at 37 °C. Cells were seeded in a 96-well plate (2×10^5 cells/ml) and cultured with the test compounds (30, 50, and 100 μM) in the presence of 100 ng/ml LPS for 24 h. Then the cells were washed with phosphate-buffered saline (PBS) and incubated with 100 μl of 0.5 mg/ml MTT [3-(4,5-dimethylthiazol-2-yl)-2,5-diphenyltetrazolium bromide] for 2 h at 37 °C to test for cell viability (Kim, Moon, Choi, Kim, & Lee, 2013). The medium was then removed and DMSO (100 μl) was added to dissolve all of the formazan crystals. The absorbance of the formazan solution was measured at 570 nm.

2.6.2. Measurement of NO production

NO production was assessed by measuring the nitrite levels in the cultured media using a colorimetric method based on the Griess reaction (Huang et al., 2013; Lai et al., 2013). The cells were seeded in a 96-well plate (2×10^5 cells/ml) and different concentrations of test compounds (5, 10, 20, 30, 50, and 100 μM) were added to the culture simultaneously with LPS (100 ng/ml)

(Sigma–Aldrich) and incubated at 37 °C for 24 h. A standard solution of $NaNO_2$ (Sigma–Aldrich) was placed in alternate wells on the same plate as well as the positive control indomethacin (Linfen Qilin Pharmaceutical Co., Ltd., Linfen, Shanxi Province, China). To quantify nitrite, 100 μl of each supernatant were mixed with the same volume of Griess reagent (1% sulphanilamide in 5% H_3PO_4 and 0.1% *N*-(L-naphthyl)ethylenediamine dihydrochloride) and incubated at room temperature for 10 min. The absorbance was measured at 540 nm, and three independent experiments were performed with each one in triplicate.

3. Results and discussion

3.1. Structure elucidation

Baeckein F (**1**) was obtained as a yellow amorphous powder. HR-ESI-MS in the positive ion mode gave a quasi-molecular ion at *m*/*z* 629.0922 $[M+H]^+$ (calcd 629.0926 for $C_{32}H_{21}O_{14}$) with an error of 0.59 ppm, which was consistent with the molecular formula of $C_{32}H_{20}O_{14}$, suggesting 23 degrees of unsaturation (Fig. S07). The IR spectrum showed absorption bands for hydroxyl group (3398 cm^{-1}), carbonyl group (1636 cm^{-1}), and aromatic functionalities (1463 cm^{-1}) (Fig. S08). The UV spectrum (λ_{max} 238, 307 and 383 nm) and the positive result for the Mg–HCl reaction suggested compound **1** to be a flavonoid.

The ^{13}C NMR spectrum (Table 1) of compound **1** displayed 32 carbon signals attributable to a carbon skeleton of biflavonoid, including two carbonyl groups (δ_C 181.0 and 176.0), two aromatic methyl groups (δ_C 6.9 and 7.2), six tertiary carbons (CH) (δ_C 119.6, 116.1, 115.6, 110.1, 98.9, and 96.3), and 22 quaternary carbons (Fig. S03). Amongst these signals, three characteristic carbons (δ_C 176.0, 147.2, and 136.4) suggested the presence of a flavonol moiety. The ^1H NMR data (Table 1) for compound **1** showed a typical ABX coupling system [δ_H 7.13 (1H, d, J = 8.7 Hz), 8.10 (1H, d, J = 2.0 Hz), and 7.91 (1H, dd, J = 8.7, 2.0 Hz)], corresponding to the 3′,4′-dihydroxy-substituted ring B of flavonoid. Also two aromatic methyl signals [δ_H 1.86 (3H, s) and 2.04 (3H, s)] and three aromatic protons [δ_H 7.09 (1H, s), 6.64 (1H, s), and 6.18 (1H, s)] were presented (Fig. S02). These above 1D-NMR data suggested compound **1** was composed of two molecules of flavonoids with structural characteristics of reported compound 6-*C*-methylquercetin (Ibewuike et al., 1996; Quang et al., 2008).

Careful inspection of the 1D-NMR and HSQC spectral data (Figs. S02–S04) of compound **1** made the assignments of one flavonoid molecule (Segment I), referring to rings A*, B*, and C*, which were confirmed by HMBC correlations (Fig. 2) from CH_3-6* (δ_H 2.04) to [δ_C 161.4 (C-5*), 102.5 (C-6*), and 160.3 (C-7*)], from H-2*′ (δ_H 7.13) to [δ_C 147.2 (C-2*), 122.0 (C-1*′), 145.4 (C-3*′), 115.6 (C-5*′), and 119.6 (C-6*′)], from H-5*′(δ_H 8.10) to [δ_C 147.2 (C-2*), 122.0 (C-1*′), 145.4 (C-3*′), 148.3 (C-4*′), and 119.6 (C-6*′)], and from H-6*′(δ_H 7.91) to [δ_C 147.2 (C-2*) and 115.6 (C-5*′)] (Fig. S05). Compared with the literature values of 6-*C*-methylquercetin (Ibewuike et al., 1996; Quang et al., 2008), the segment I was further identified, but the absence of an H-8* signal revealed a substituted C-8*, suggesting one available binding position for the other flavonoid molecule (Segment II).

In the ^1H NMR spectrum of compound **1**, the aromatic methyl [δ_H 1.86 (3H, s, CH_3-6)] and one aromatic proton [δ_H 6.18 (1H, s, H-8)] assignable to a ring A of 6-*C*-methylquercetin, and the remaining two aromatic protons [δ_H 6.64 (1H, s, H-3′) and 7.09 (1H, s, H-6′)] attributable to a 1′,2′,4′,5′-tetrasubstituted ring B of flavonoid, indicated the presence of rings A and B in the segment II, respectively. In the ^{13}C NMR spectrum of compound **1**, the carbonyl carbon [δ_C 181.0 (C-4)] and two quaternary carbons [δ_C 111.6 (C-2) and 93.8 (C-3)] revealed that the carbon skeleton of

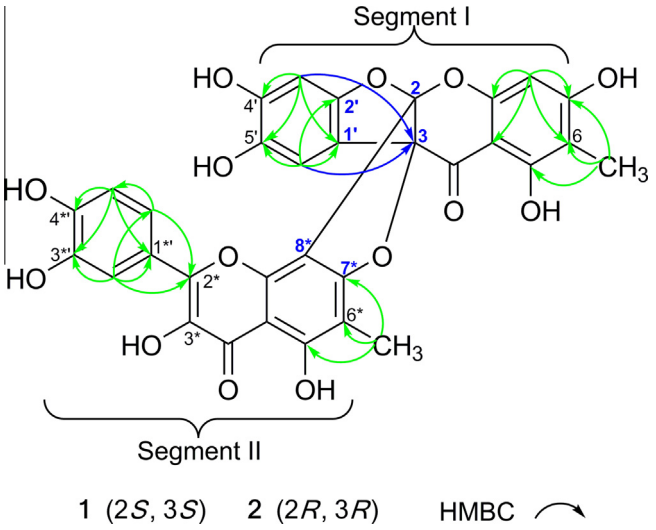

Fig. 2. Selected HMBC correlations for compounds **1**–**2**.

ring C in the segment II should be a dihydropyrone ring, different from the pyrone ring C of 6-*C*-methylquercetin. In addition, new substituents must be bound to the carbons C-2 and C-3, suggesting two available binding positions for the segment I. The distinctive chemical shifts [δ_C 111.6 (C-2), 93.8 (C-3), 149.1 (C-2′), 150.4 (C-4′), and 142.1 (C-5′)] indicated that each of the five quaternary carbons should be bearing oxygen atoms. Consequently, a furan ring between rings B and C was proposed according to the number of oxygen atoms in the established molecular formula. And the furan ring D was confirmed by evident cross-peaks from H-3′ and H-6′ to C-3 (instead of C-2) in the HMBC spectrum. Also the segment II, referring to rings A–D was confirmed by HMBC correlations (Fig. 2) from CH_3-6 to [δ_C 161.6 (C-5), 105.6 (C-6), and 167.7 (C-7)], from H-8 to [δ_C 181.0 (C-4), 105.6 (C-6), 167.7 (C-7), 156.8 (C-9), and 100.0 (C-10)], from H-3′ to [δ_C 93.8 (C-3), 115.2 (C-1′), 150.4 (C-4′), 142.1 (C-5′), and 110.1 (C-6′)], and from H-6′ to [δ_C 93.8 (C-3), 115.2 (C-1′), 149.1 (C-2′), 98.9 (C-3′), and 142.1 (C-5′)] (Fig. S05). Furthermore, the furan ring D, resulting from the unusual connections between rings B and C, was further verified by the related NMR data of known compounds daphnodorins E and G (Baba, Yoshikawa, Taniguchi, & Kozawa, 1994; Taniguchi & Baba, 1996).

The above spectral analysis indicated that the carbons C-2, C-3, and C-8* provided three available binding positions for segments I and II. Comparative evaluation of the chemical shifts for C-2, C-3, and C-8* revealed that the C-2 was bound to the aromatic carbon C-8* and the C-3 should be bound to another oxygen atom. Accordingly, the C-2–C-8* bond and the C-3–O–C-7* linkage were deduced from these pieces of evidence together with the molecular weight and the remaining degrees of unsaturation. It was interesting that the optimal connections C-2–C-8* and C-3–O–C-7* between the two segments formed a furan ring E. And the unusual furan ring E was verified by comparison of the experimental NMR data with the values simulated by ACD Labs software. As a result, the planar structure for compound **1** was determined.

In the molecule of compound **1**, the carbons C-2 and C-3 provided two chiral centres, and there were three planes referring to rings C–E around the central axis of the C-2–C-3 bond. As the plane formed by rings A and C was taken for a reference, the relative stereochemistry of rings D and E could be assigned as (2*R*,3*R*) or (2*S*,3*S*). It was unfortunate that our NOESY experiment did not give useful NOE increments for the stereochemical assignments (Fig. S06), and also the CD spectrum (Fig. 3-A1) of compound **1**

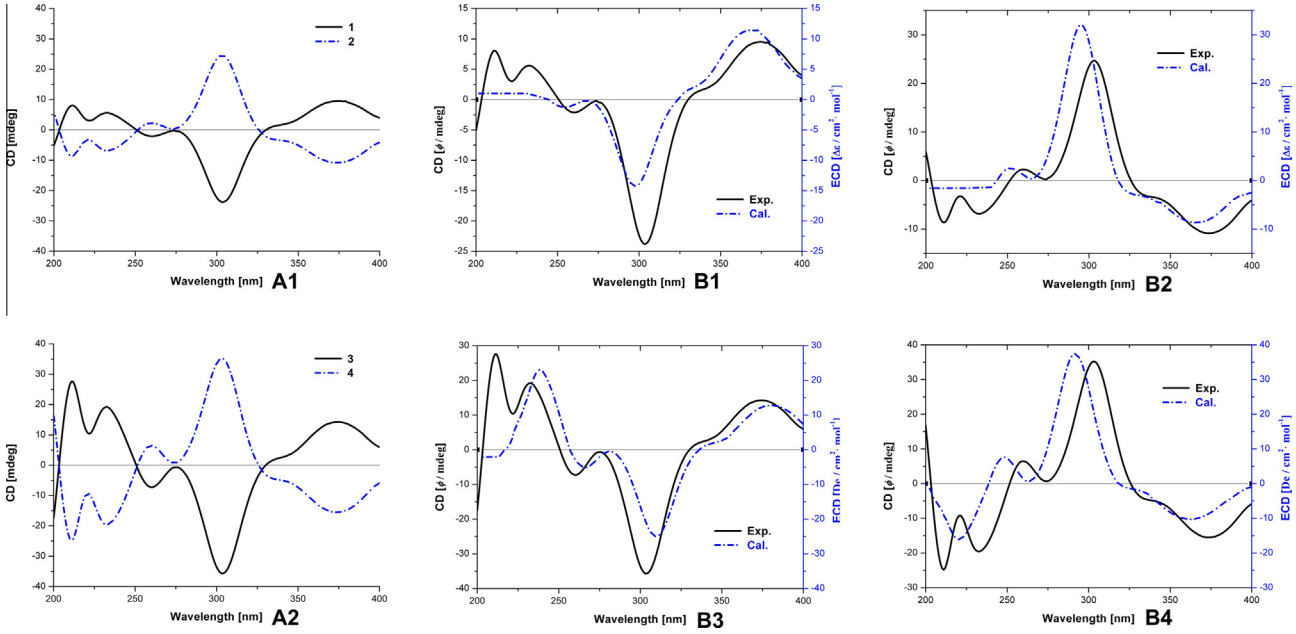

Fig. 3. Experimental CD (A1–A2) and calculated CD (B1–B4) spectra for compounds **1**–**4**.

showing positive Cotton effects (CEs) at 211, 233 and 379 nm, and negative CEs at 260 and 304 nm, was not sufficient enough to determine the absolute configurations of the C-2 and C-3. In this case, quantum chemical CD calculations were employed (Jia, Zhou, et al., 2011, 2013). The geometry was built on the 3D-structure of compound **1** with the given configurations (2*S*,3*S*). The conformational analysis was performed by means of the semi-empirical PM3 method, as implemented in the Q-Chem programme package, starting from pre-optimised geometries generated by the MM2 force field in the Chem 3D software. The electronic circular dichroism (ECD) spectrum was computed in the gas phase using the TD-DFT at the B3LYP/6-31G+ (d,p) level. The calculated CD spectrum (Fig. 3-B1) displayed diagnostic negative CEs and positive CEs, which exhibited good agreements with the experimental CD, and allowed the assignments of the absolute configurations of **1** as depicted. On the basis of these above results, the structure of baeckein F (**1**) was unambiguously established.

Baeckein G (**2**) was also obtained as a yellow amorphous powder and possessed the molecular formula of $C_{32}H_{20}O_{14}$, as established by HR-ESI-MS (*m*/*z* 627.0794 [M−H]$^-$, calcd 627.0780 for $C_{32}H_{19}O_{14}$) (Fig. S14). Comprehensive analysis of the ^{1}H/^{13}C NMR data (Table 1) and 2D-NMR correlations (Fig. 2) disclosed that compound **2** shared the same planar structure with compound **1**, suggesting a pair of enantiomers (Figs. S09–S13). And this deduction was verified by the CD spectrum (Fig. 3-A1) of compound **2**, exhibiting positive CEs at 260 and 303 nm, and negative CEs at 211, 233 and 374 nm, almost a mirror image for the CD spectrum of compound **1**. Meanwhile, a TD-DFT calculation for the ECD data of compound **2** was also carried out following the same procedures that compound **1** used. It was fortunate that the shapes of the calculated CD and experimental CD spectra of compound **2** were nearly the same (Fig. 3-B2). Accordingly, the absolute stereochemistry for chiral carbons of C-2 and C-3 in compound **2** was assigned as (2*R*,3*R*).

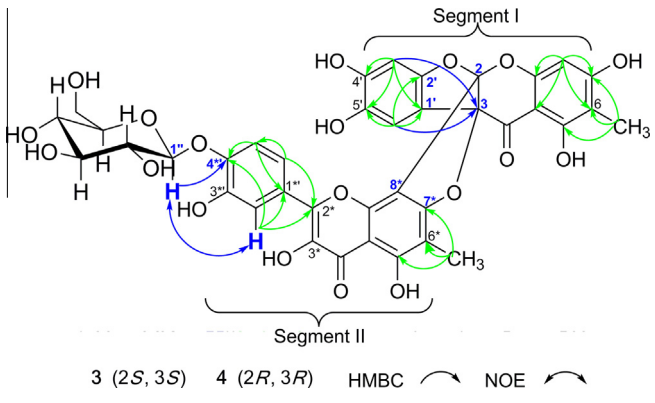

Fig. 4. Selected HMBC and NOE correlations for compounds **3**–**4**.

Baeckein H (**3**) was isolated as a yellow amorphous solid and gave the quasi-molecular ion peak [M−H]$^-$ at *m*/*z* 789.1313 (calcd 789.1308 for $C_{38}H_{29}O_{19}$, 0.57 ppm), consistent with the elemental composition $C_{38}H_{30}O_{19}$ (Fig. S20). Its IR spectrum showed absorption bands for hydroxyl (3397 cm^{-1}), carbonyl (1635 cm^{-1}) and aromatic functionalities (1508 and 1463 cm^{-1}) (Fig. S21). The UV spectrum (λ_{max} 228, 308 and 380 nm) and positive results for the Mg–HCl reaction and Molisch reagent, and the chemical formula suggested compound **3** to be a biflavonoid glycoside. The ^{13}C NMR spectrum of compound **3** (Table 1) displayed a group of signals (δ_C 101.6, 77.2, 75.9, 73.3, 69.8, and 60.8) belonging to a hexosyl unit, and 32 carbon signals attributable to a carbon skeleton of biflavonoid, amongst which were two carbonyl groups (δ_C 181.1 and 176.3), two aromatic methyl groups (δ_C 6.9 and 7.2), six CH (δ_C 119.4, 116.2, 115.3, 110.0, 98.9, and 96.2), and 22 quaternary carbons (Fig. S16). The ^{1}H NMR spectrum (Table 1) of compound **3** showed a typical ABX coupling system [δ_H 7.44 (1H, d, *J* = 8.7 Hz), 8.10 (1H, d, *J* = 2.0 Hz), and 7.96 (1H, dd, *J* = 8.7, 2.0 Hz)], two aromatic methyl signals [δ_H 1.83 (3H, s) and 2.00 (3H, s)], three aromatic protons [δ_H 7.05 (1H, s), 6.61 (1H, s), and 6.13 (1H, s)], and a series of signals in the range of δ_H 5.0–3.0 related to a sugar moiety (Fig. S15). A comparison of the 1D-NMR data of compound **3** with those of **1** suggested that compounds **1** and **3** had the same carbon skeleton and functional groups, except for the signals assignable to a hexosyl moiety. The planar structure for the aglycone part of compound **3**, including the segments I and

Table 2
NO inhibitory effects and cytotoxic activities of compounds **1**–**4**.

Compounds	IC_{50} (μM) (mean ± SD, n = 3)	
	Inhibitory effects	Cytotoxicity
1	54.7 ± 5.26	>100
2	25.4 ± 2.78	>100
3	43.8 ± 3.30	>100
4	15.2 ± 1.34	>100
Indomethacin	13.8 ± 1.29	>100

II, was the same as that of **1**, which was confirmed by the HMBC experiment (Figs.4 and S18). The sugar moiety was identified as D-glucose by TLC and GC analysis after the acid hydrolysis experiment of compound **3** (Hao et al., 2008; Tang et al., 2005). The large $^3J_{H\text{-}1,H\text{-}2}$ coupling constant of the anomeric proton [δ_H 4.94 (1H, d, J = 7.0 Hz, H-1″)] revealed that the β-configuration for the glucose moiety, and the location of the glucose residue being at C-4*′ was confirmed by the HMBC cross-peak from H-1″ to C-4*′ (δ_C 161.6) and the NOE correlation (Fig. 4) between H-1″and H-2*′ [δ_H 7.50 (1H, s)] (Fig. S19). Furthermore, the β-D-glucose moiety was verified by related data in the literature (Quang et al., 2008). Finally, the absolute stereochemistry for the quaternary carbons C-2 and C-3 in compound **3** was assigned as (2*S*,3*S*) by comparison of the characterised shapes in computed CD (Fig. 3-B3) with those in the experimental CD (Fig. 3-A2) spectra, which displayed positive CEs at 211, 232, and 375 nm, and negative CEs at 260 and 304 nm.

Baeckein I (**4**) was also isolated as a yellow amorphous solid and a quasi-molecular ion $[M+H]^+$ at m/z 791.1455 (calc. 791.1454 for $C_{38}H_{31}O_{19}$, −0.09 ppm) in the HR-ESI-MS suggested a molecular formula of $C_{38}H_{30}O_{19}$ (Fig. S27). The $^1H/^{13}C$ NMR data (Table 2) and 2D correlations (Fig. 4) suggested that the planar structure for the aglycone part of compound **4** and the β-D-glucose unit at C-4*′ were the same as those of compound **3**, indicating a pair of diastereoisomers (Figs. S22–S26). The experimental CD spectrum (Fig. 3-A2) for compound **4** showed positive CEs at 260 and 304 nm, and negative CEs at 211, 233, and 374 nm. Also the absolute stereochemistry for the chiral centres of C-2 and C-3 in compound **4** was assigned as (2*R*,3*R*) by the TD-DFT calculations used above.

3.2. Anti-inflammatory activity

The anti-inflammatory activities for baeckeins F–I (**1**–**4**) (above 95% purity) were evaluated by detecting the NO productions of LPS-induced RAW264.7 cell line (Huang et al., 2013; Lai et al., 2013). The concentration required to inhibit NO production by 50% (IC_{50}) was calculated on the basis of concentrations of nitrite released into the culture media with the Griess method. The cell viability was examined by the MTT assay to ascertain if NO inhibition was due to the cytotoxicity of test compounds. The IC_{50} values for compounds **1**–**4** were summarised in Table 2, suggesting that all test compounds possessed dose-dependent NO inhibitory effects in the concentration range of 5–100 μM, but with no cytotoxic activities on the RAW264.7 macrophages (Table S01). It was interesting that the absolute configurations of (2*R*,3*R*) for compounds **2** and **4** significantly enhanced the NO inhibitory effects, compared to the configurations of (2*S*,3*S*) for compounds **1** and **3**, and compounds **3** and **4** with the β-D-glucose moiety were more active than compounds **1** and **2** without any sugar residues. The improved inhibitory effects resulting from the absolute stereochemistry were much greater than those from the β-D-glucose unit. Accordingly, compound **4** exhibited the highest inhibitory activity with an IC_{50} of 15.2 μM, which was similar to the positive control, indomethacin (IC_{50} = 13.8 μM).

4. Conclusions

The present study provided another four unusual *C*-methylated biflavonoids following the reported compounds baeckeins A–E. From a chemical point of view, the unique carbon skeleton for baeckeins F–G (the aglycone) could be regarded as the first conjugates of a flavonol (the segment I) and one coumaronochromone molecule (the segment II) via the unusual linkages of C-2–C-8* and C-3–O–C-7*, whilst baeckeins H–I were the corresponding glucopyranosides. Absolute configurations for chiral carbons of C-2 and C-3 were determined by the CD spectrum combined with quantum chemical calculations (TD-DFT). Preliminary studies on the structure–activity relationships revealed that the glucopyranose unit and configurations of (2*R*,3*R*) were two important factors responsible for anti-inflammatory activities, but the detailed mechanism of action should be investigated in future. These results herein have provided additional phytochemical and bioactive information for resource development and utilisation of *B. frutescens* for food and health purposes, and the *C*-methylated flavonoids might be good candidates for anti-inflammatory agents.

Acknowledgements

This work was supported by the National Natural Science Foundation of China (81303162) and the Priority Academic Program Development of Jiangsu Higher Education Institutions (PAPD). We appreciate the kind help from Dr. Xiao-Bing Wang (Department of Natural Medicinal Chemistry, China Pharmaceutical University) for providing assistance in the quantum chemical CD calculations and Mr. Mao-Xiang Lai (Guangxi Academy of Chinese Medicines and Pharmaceutical Science) for collecting the plant materials.

Appendix A. Supplementary data

Supplementary data associated with this article can be found, in the online version, at http://dx.doi.org/10.1016/j.foodchem.2014.01.022.

References

Baba, K., Yoshikawa, M., Taniguchi, M., & Kozawa, M. (1994). Biflavonoids from *Daphne Odora*. *Phytochemistry, 38*(4), 1021–1026.
Frisch, M. J., Trucks, G. W., Schlegel, H. B., Scuseria, G. E., Robb, M. A., Cheeseman, J. R. Jr.,, et al. (2010). *Gaussian 10 user's reference*. Wallingford, CT: Gaussian Inc.
Fujimoto, Y., Usui, S., Makino, M., & Sumatra, M. (1996). Phloroglucinols from *Baeckea frutescens*. *Phytochemistry, 41*(3), 923–925.
Gottlieb, O. R., Da Silva, M. L., & Maia, J. G. S. (1972). Eucalyptin from *Eugenia* and *Myrcia* species. *Phytochemistry, 11*(3), 1185–1189.
Hao, G., Zhao, W., Lei, Y., Yang, Y., Yao, Z. H., Wang, N. L., et al. (2008). Five new bidesmoside triterpenoid saponins from *Stauntonia chinensis*. *Magnetic Resonance in Chemistry, 46*(7), 630–637.
Huang, S., Zhou, X. L., Wang, C. J., Wang, Y. S., Xiao, F., Shan, L. H., et al. (2013). Pyrrolizidine alkaloids from *Liparis nervosa* with inhibitory activities against LPS-induced NO production in RAW264.7 macrophages. *Phytochemistry, 93*, 154–161.
Ibewuike, J. C., Ogundaini, A. O., Ogungbamila, F. O., Martin, M. T., Gallard, J. F., Bohlin, L., et al. (1996). Piliostigmin, a 2-phenoxychromone, and C-methylflavonols from *Piliostigma thonningii*. *Phytochemistry, 43*(3), 687–690.
Jantan, I., Ahmad, A. S., Bakar, S. A. A., Ahmad, A. R., Trockenbrodt, M., & Chak, C. V. (1998). Constituents of the essential oil of *Baeckea frutescens* L. from Malaysia. *Flavour and Fragrance Journal, 13*(4), 245–247.
Jia, B.-X., Ren, F.-X., Jia, L., Chen, X.-Q., Yang, J., & Wang, Q. (2013). Baeckein E, a new bioactive *C*-methylated biflavonoid from the roots of *Baeckea frutescens*. *Natural Product Research, 27*(22), 2069–2075.
Jia, B.-X., Yang, J., Chen, X.-Q., Cao, Y., Lai, M.-X., & Wang, Q. (2011). Baeckeins A and B, two novel 6-methylflavonoids from the roots of *Baeckea frutescens*. *Helvetica Chimica Acta, 94*(12), 2283–2288.
Jia, B. X., Zhou, Y. X., Chen, X. Q., Wang, X. B., Yang, J., Lai, M. X., et al. (2011). Structure determination of baeckeins C and D from the roots of *Baeckea frutescens*. *Magnetic Resonance in Chemistry, 49*(11), 757–761.

Kamiya, K., & Satake, T. (2010). Chemical constituents of *Baeckea frutescens* leaves inhibit copper-induced low-density lipoprotein oxidation. *Fitoterapia, 81*(3), 185–189.

Kim, K. H., Moon, E., Choi, S. U., Kim, S. Y., & Lee, K. R. (2013). Polyphenols from the bark of *Rhus verniciflua* and their biological evaluation on antitumor and anti-inflammatory activities. *Phytochemistry, 92*(4), 113–121.

Lai, P. K.-K., Chan, J. Y.-W., Wu, S.-B., Cheng, L., Ho, G. K.-W., Lau, C.-P., et al. (2013). Anti-inflammatory activities of an active fraction isolated from the root of *Astragalus membranaceus* in RAW 264.7 macrophages. *Phytotherapy Research* (Epub ahead of print).

Makino, M., & Fujimoto, Y. (1999). Flavanones from *Baeckea frutescens*. *Phytochemistry, 50*(2), 273–277.

Mayer, R. (1990). Flavonoids from *Leptospermum scoparium*. *Phytochemistry, 29*(4), 1340–1342.

Pan, Z.-B., Li, F.-C., Liao, Y.-E., & Lin, X.-S. (2012). Antioxidant activity and anti-inflammatory effect of total flavonoids from *Baeckea frutescen*. *China Pharmacist, 15*(4), 477–478.

Quang, T. H., Cuong, N. X., Minh, C. V., & Kiem, P. V. (2008). New flavonoids from *Baeckea frutescens* and their antioxidant activity. *Natural Product Communications, 3*(5), 755–758.

Rao, J. R., & Rao, R. S. (1991). Syzalterin, a new 6,8-di-C-methyflavone from *Syzygium alternifolium* leaves. *Indian Journal of Chemistry B, 30*(1), 66–67.

Satake, T., Kamiya, K., Saiki, Y., Hama, T., Yasuo, F., Endang, H., et al. (1999). Chromone C-glycosides from *Baeckea frutescens*. *Phytochemistry, 50*(2), 303–306.

Tam, N. G. T., Thuam, D. T., Bighelli, A., Castola, V., Muselli, A., Richomme, P., et al. (2004). *Baeckea frutescens* leaf oil from Vietnam: Composition and chemical variability. *Flavour and Fragrance Journal, 19*(3), 217–220.

Tang, L., Jiang, Y., Chang, H. T., Zhao, M. B., Tu, P. F., Cui, J. R., et al. (2005). Triterpene saponins from the leaves of *Ilex kudingcha*. *Journal of Natural Products, 68*(8), 1169–1174.

Taniguchi, M., & Baba, K. (1996). Three biflavonoids from *Daphne Odora*. *Phytochemistry, 42*(5), 1447–1453.

Tsui, W.-Y., & Brown, G. D. (1996a). Sesquiterpenes from *Baeckea frutescens*. *Journal of Natural Products, 59*(11), 1084–1086.

Tsui, W.-Y., & Brown, G. D. (1996b). Chromones and chromanones from *Baeckea frutescens*. *Phytochemistry, 43*(4), 871–876.

Tsui, W.-Y., & Brown, G. D. (1996c). Unusual metabolites of *Baeckea frutescens*. *Tetrahedron, 52*(29), 9735–9742.

Wollenweber, E., Wehde, R., Dörr, M., Lang, G., & Stevens, J. F. (2000). *C*-methyl-flavonoids from the leaf waxes of some Myrtaceae. *Phytochemistry, 55*(8), 965–970.